Integration, the VLSI Journal 64 (2019) 50–59

Contents lists available at ScienceDirect

Integration, the VLSI Journal

journal homepage: www.elsevier.com/locate/vlsi

# An accurate classifier based on adaptive neuro-fuzzy and features selection techniques for fault classification in analog circuits

Abderrazak Arabi [a,*], Nacerdine Bourouba [a], Abdesslam Belaout [b], Mouloud Ayad [c]

[a] Laboratory of Scientific Instrumentation (LIS), Faculty of Technology, Ferhat Abbas Sétif 1 University, 19000, Sétif, Algeria
[b] Laboratory of Power Electronics and Industrial Control (LEPCI), Faculty of Technology, Ferhat Abbas Sétif 1 University, 19000, Sétif, Algeria
[c] Electrical Engineering Department, Faculty of Sciences and Applied Sciences, Bouira University, 10000, Bouira, Algeria

ARTICLE INFO

*Keywords:*
Analog circuits
Fault detection
Fault classification
Neuro-fuzzy classifier
Features reduction

ABSTRACT

This paper presents a new approach for faults classification in analog integrated circuits using a multiclass adaptive neuro fuzzy inference system classifier. This is carried out to assist analog circuit's faults diagnosis suffering from inaccurate faults classification on one hand, and to lessen computational burden on the other hand. This has been achieved from features number reduction. These features serving as input feature vector are extracted from the selected circuits (CUT) frequency and transient responses under both fault free and faulty conditions. The considered faults are resistors and capacitors values variations of about 50% low and high from their nominal ones. The method accuracy has been validated with three experiment circuits, the Sallen Key band-pass, the four opamp biquad high-pass and the leapfrog filters. The obtained results reveal a high level of efficiency with an accuracy average reach to 99.76%. Hence, the proposed method has shown a good performance in term of fault classification accuracy when compared with those of both the Artificial Neural Networks (ANN) approach and the fractional Fourier transform (FRFT) method based on a statistical property.

## 1. Introduction

Due to the poor fault models, component tolerances and the circuits' nonlinear behavior, the fault diagnosis of analog integrated circuits becomes more complicated. Therefore, the development of efficient methods for fault detection and classification in analog circuits still the main needed project of many researchers.

The fault diagnosis systems main functions are fault detection, fault isolation, Fault identification, Fault prediction, Fault explanation and Fault simulation [1]. Feature extraction methods are strictly related to the efficiency of fault diagnosis for analog circuits.

Hard faults and soft faults are the main categories of faults in analog circuits. The first ones are also known as catastrophic faults, whereas soft faults are considered as parametric faults [1], more details are given in section 2. However, the research proposals are dealing mostly with the parametric fault detection since the second category faults are difficult to detect. But it becomes easy to locate hard faults, to isolate and to correct them as well. In this perspective, there are two approaches of analog circuits fault diagnosis: the simulation before test approach (SBT) and the simulation after test approach (SAT). In the SAT attitude, fault diagnosis is obtained by extracting the circuit parameters from the CUT measured responses. The SBT approach compares the CUT responses with the predefined fault values in the fault dictionary, and thus helping to locate the faults. Besides, this approach has confirmed a test and computing time reduction even for complex circuits that, unfortunately the other approach (SAT) is still suffering of the lack of this performance. Furthermore, fault detection and fault isolation are achieved by means of a classification system which provides a decision based on deviations between the actual CUT responses and the stored ones.

Different methods for fault detection and classification were proposed in various literature. For instance, the authors in literature [2] have developed a statistical property feature extraction based on FRFT. In this method, optimal features were derived using Kernel principal component analysis (KPCA), and support vector machine (SVM) to diagnose faulty components in analog circuits. The literature [3] has dealt with a Fuzzy Inference System (FIS) constructed to model and classify faults in analog

* Corresponding author.
*E-mail addresses:* arabi_abderrazak@yahoo.fr (A. Arabi), bourouband@yahoo.fr (N. Bourouba), belaout.abdesslam@univ-setif.dz (A. Belaout), ayad_moul@yahoo.fr (M. Ayad).

https://doi.org/10.1016/j.vlsi.2018.08.001
Received 20 March 2018; Received in revised form 30 July 2018; Accepted 2 August 2018
Available online 18 August 2018

circuits. Then, hybrid neuro-fuzzy systems were also built and trained to isolate faults of the CUT. The authors of [4] have presented the Neuro-Fuzzy System to Time Domain for fault diagnosis of electronic circuits. The proposed neural network classifier has aimed to solve the problem of distinguishing between healthy and faulty circuit. Hence, a neural dictionary was created to locate fault and fuzzy logic was used to translate a measurement vector into a zero-one range for fault classification. Another research work of has proposed a fuzzy classifier to provide single and multiple fault diagnosis with the variation in the components value below ±50% [5]. This technique was based on three signature parameters: peak gain, its frequency and its phase of the CUT frequency response were used as features to train classifier. Some fault diagnosis methods are based on signal processing. The authors have proposed in here a fractional wavelet transform technique (FWT) to extract fault features [6]. A fuzzy multi-classifier based on the Support Vector Data Description (SVDD) has been adopted to diagnose faults in analog circuits.

Multi frequency approach has been optimized for fault diagnosis [7]. Consequently, both the test frequencies number for fault diagnosis and the simulation time required have been reduced. Authors in Ref. [8] propose wavelet transform coefficients as features to train classifier. Generally, feature extraction and classifier application represent the main steps of the data driven methods, such as neural networks (ANNs) and support vector machines (SVMs), to locate the faults [9]. In Ref. [10], transient feature extraction approach using the optimized Morlet wavelet transform was proposed to solve the problem in the weak transient detection. Authors in Ref. [11] propose a method for faults diagnosis in analog circuits, using features extracted from the time frequency responses and an improved vector-valued regularized kernel function approximation (VVRKFA).

In fact, many other methods can be found in a wide and various literature. They all of them deal with a same target of finding an accurate fault classifier but involving different approaches such as a digital signature analysis [12], A statistical approach [13], BP neural networks [14], the hybrid evolutionary algorithm and neural network use [15], network parameters and neural networks [16,17].

In this paper, a novel fault detection and classification approach is proposed. Classifier features were extracted from the frequency and the transient responses for the classifier training. The features number was reduced by using variable dimensionality reduction technique to lessen time of the classifiers requirement.

The novel contribution of this study is to integrate the appropriate membership function type with their number optimization, and input features reduction to achieve a high accuracy classification. This method is validated through a Sallen-Key band-pass filter, a four op-amp biquad high-pass filter and a leapfrog filter.

The paper is organized as follows: section 2 presents the main types of faults in analog circuits. The neuro-fuzzy classifier development and the concept of the proposed classifier with two inputs (binary) are given in section 3. Section 4 discusses the simulation result of the experiment circuits. Section 5 exhibits the experimental results and discussion about the proposed constructed classifier and its features reduction achievement. This has been followed by the actual classifier approach efficiency evaluation and comparing it with those of the ANN's and the statistical property based FRFT method classifier. Finally, section 6 concludes the proposed classifier method along with future work.

## 2. Faults in analog integrated circuits

Faults in the analog integrated circuits are classified into two categories: hard faults and soft faults [1]. Hard faults are also known as catastrophic faults, In this case, the faulty component may be short circuited, open circuited or apparition of large deviation in the circuit elements design parameter. Hard faults are generally caused by the electromigration and particle contamination phenomena occurrence in the conducting and metallization layers.

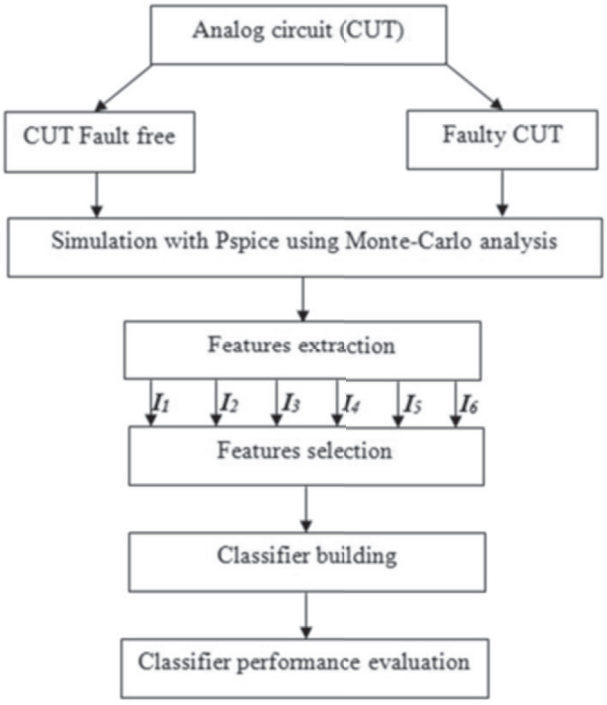


**Fig. 1.** Process of fault classifier building for fault classification in the CUT.

Soft faults are also called parametric faults. This fault type is caused by element value change or its deviation from the nominal values. The presence of these faults in the analog circuits degrades the performance of the circuit. The deviation recorded on the component nominal value which is out of the tolerance band is attributed to either the circuit ageing, or manufacturing tolerances or parasitic effects in the circuits.

According to both the faults number and their occurrence, faults in analog integrated circuits are mainly categorized into two types: single faults and multiple faults. However, the huge amount of work that the study of the whole types of faults will require has driven us to focus our attention on single faults while the second fault type is left for future work.

## 3. Neuro-fuzzy classifier building

Adaptive Neuro Fuzzy Interface System (ANFIS) is one of the greatest trades off among ANNs and fuzzy logic systems. They offer smoothness owing to the interpolation and adaptability of fuzzy control and to the ANN back propagation. ANFIS provides a technique for the fuzzy modeling procedure to attain information about a data set, in order to compute the membership function parameters that best allow the associated fuzzy inference system to track the given input/output data [3]. ANFIS is a class of ANN, which is based on fuzzy interface system and incorporates both ANN and fuzzy logic principles and has benefits of both techniques in a single framework. The necessary steps for the process of neuro fuzzy classifier are illustrated in Fig. 1:

- Simulation Monte-Carlo of the CUT under fault and fault free conditions;
- Features extraction;
- Features reduction;
- Classifiers training and testing;
- Classifiers synthesis and final decision.

### 3.1. Neuro-fuzzy classifier principal

Fuzzy systems are able to hold uncertain and inaccurate information,

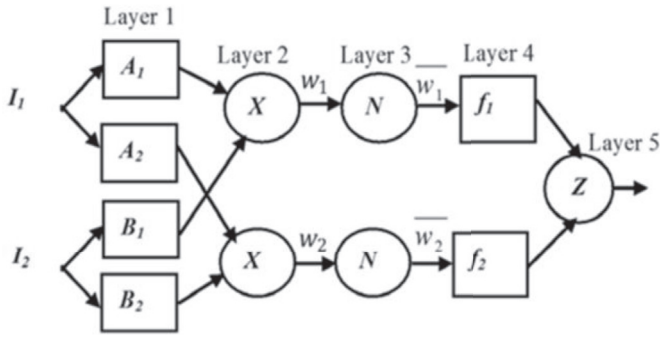


**Fig. 2.** ANFIS architecture model with two inputs, one output and two rules.

but cannot update and fine tune their parameters automatically. To overcome this disadvantage, a neural network learning algorithms were applied, by training data set [19]. A Sugeno-type fuzzy Inference System (FIS) is used, whose the consequent is constant: this FIS type is known as zero-order Sugeno type [20].

The applied neuro-fuzzy system procedure as depicted in Fig. 2 uses a simple architecture. To explain the procedure principle, we assume the ANFIS structure has two inputs, with maximum amplitude of frequency response (I1) and its center frequency (I2) as input features, and one output (Z) representing a fault class. In case of two existing rules only and according to the zero-order Sugeno type classifier, outputs are computed by summing of two functions ($f_1$ , $f_2$) as follow:

- $f_1$: is computed by the rule:

  If $I_1$ is $A_1$ and $I_2$ is $B_1$, then

$$f_1 = p_{11} \times I_1 + p_{12} \times I_2 + r_1 \tag{1}$$

- $f_2$: is computed by the rule:

  If $I_1$ is $A_2$ and $I_2$ is $B_2$, then

$$f_2 = p_{21} \times I_1 + p_{22} \times I_2 + r_2 \tag{2}$$

where *Ai* and *Bi* are the fuzzy sets, *fi* is the output, $p_{ij}$ and $r_i$ ($i = j = 1, 2$), are the consequents parameters. The ANFIS architecture used to implement the two rules is shown in Fig. 2. Squares represent adaptive nodes, where circles represent the fixed nodes.

The structure of ANFIS includes five layers that can be described as follows:

a) Layer 1: Features layer

For this layer, the output of the node i is calculated by the equations:

$$O_i^1 = \mu_{A1}(I_1) \text{ for } i = 1, 2 \tag{3}$$

Or

$$O_i^1 = \mu_{B-2}(I_2) \text{ for } i = 1, 2 \tag{4}$$

where, $I_1$ and $I_2$ are the crisp features that feed the input of the node i. $A_i$ and $B_i$ are linguistic terms related with their proper membership functions, characterized by appropriate membership functions $\mu_{Ai}$ and $\mu_{Bi-2}$, respectively. $O_i^1$ is the output of the $i_{th}$ node of the layer. Membership functions for linguistic terms can be any appropriate membership functions. In this example, trapezoidal membership functions are used.

$$\mu_{A_i} = \begin{cases} 0, & I_1 \le a_i \\ \dfrac{I_1 - a_i}{b_i - a_i}, & a_i \le I_1 \le b_i \\ 1, & b_i \le I_1 \le c_i \\ \dfrac{d_i - I_1}{d_i - c_i}, & c_i \le I_1 \le d_i \\ 0, & d_i \le I_1 \end{cases} \tag{5}$$

$$\mu_{B_i} = \begin{cases} 0, & I_2 \le a_i \\ \dfrac{I_2 - a_i}{b_i - a_i}, & a_i \le I_2 \le b_i \\ 1, & b_i \le I_2 \le c_i \\ \dfrac{d_i - I_2}{d_i - c_i}, & c_i \le I_2 \le d_i \\ 0, & d_i \le I_2 \end{cases} \tag{6}$$

where $\mu_{Ai}$ and $\mu_{Bi}$ are the membership functions. *ai, bi, ci* and *di* are the parameters that change by the training algorithm to arrangement with training data set. Hence, the trapezoidal function varies consequently.

b) Layer 2: Rules layer

In this layer, the nodes provide a sacking strength $O_i^2$, and it is the product of all outputs resulted from layer one. No parameter to be adjusted, so it represents a fixed node.

$$O_i^2 = w_i = \mu_{A_i}(I_1)\, \mu_{B_i}(I_2), \quad i = 1, 2 \tag{7}$$

c) Layer 3: Normalization layer

The node i of the normalization layer takes the ratio of the $i_{th}$ rule's firing strength to the sum of all rule's firing strengths. The outputs of this layer are called normalized firing strength.

$$O_i^3 = \overline{w_i} = \frac{w_i}{\sum_i w_i}, \quad i = 1, 2 \tag{8}$$

d) Layer 4: Consequent layer

Every node *i* in this layer is an adaptive node. The node function of the fourth layer computes the contribution of each ith rule's toward the total output. The output of the node *i* of this layer is computed by the following function:

$$O_i^4 = \overline{w_i} f_i \quad i = 1, 2 \tag{9}$$

where, $\overline{w_i}$ is a normalized firing strength from the layer 3. The formulas that compute $f_i$ are given in equation (1) and equation (2).

e) Layer 5: Output layer

The single node in this layer is a fixed node labeled sum and computes the overall output as the summation of all incoming signals. Therefore, the process of Defuzzification is achieved by getting a crisp general output.

$$O_i^5 = \sum_i \overline{w_i} f_i = \frac{\sum_i w_i f_i}{\sum_i w_i}, \quad i = 1, 2 \tag{10}$$

We note that the above described ANFIS classifier is just an example. In the following we will use more inputs and more rules will be also generated using learning algorithms.

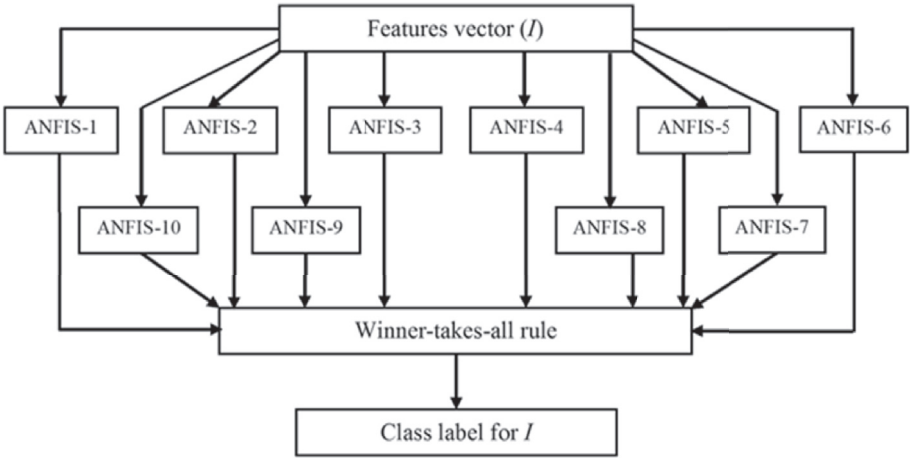


**Fig. 3.** Concept of multiclass neuro-fuzzy classifier.

### 3.2. Multiclass classification approach

In this study, we can use a collection of classifiers that is called multiclass classification. In this case, results decisions are compared by using "winner-takes-all" rule as presented in Fig. 3. Each classifier feed this rule by a crisp class label which is assigned to the output (Z). The final class label of Z is the one that have the major crisp value at the outputs of the classifiers group.

If the result at the classifier output *i*, is *di* then the label L at the output of the over mentioned rule is computed by:

$$L = \max(d_i) \tag{11}$$

### 3.3. Classifiers performance evaluation criterions

The classifier performance will be evaluated by using two statistical criterions: root mean squared error and correlation coefficient. This allows us to compare it to other type of classifier.

The root mean squared error (RMSE) is given by the following expression:

$$RMSE = \sqrt{\frac{\sum_{i=1}^{n}(m_i - p_i)^2}{n}} \tag{12}$$

The correlation coefficient ($R^2$) is given by the following expression:

$$R^2 = 1 - \frac{SSE}{\sum_{i=1}^{n} p_i^2} \tag{13}$$

where (SSE) represents a sum square error that is given by the following expression:

$$SSE = \sum_{i=1}^{n}(m_i - p_i)^2 \tag{14}$$

$m_i$ is the actual value, $P_i$ is the predicted output of the classifier, and n is the number of inputs data.

## 4. Example circuits and experiment simulation results

The proposed fault classification system employed to detect and classify faults of analog circuits is validated by three example circuits, a Sallen–Key band-pass filter, a four opamp biquad high-pass filter and a leapfrog filter. In this study, single parametric faults have only been considered.

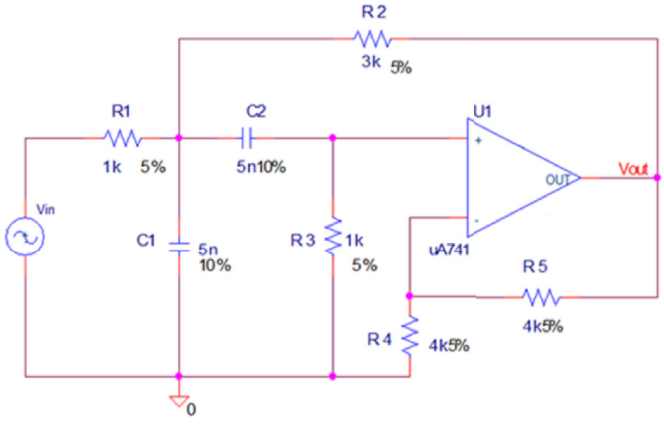


**Fig. 4.** Sallen-Key band pass filter circuit.

**Table 1**
Nominal and fault values for a Sallen-Key band pass filter.

| Fault ID | Element | Nominal value | Fault type | Faulty value |
|---|---|---|---|---|
| F0 | – | – | FF | |
| F1 | R1 | 1 kΩ | R1+50% | 1.5 kΩ |
| F2 | R1 | 1 kΩ | R1-50% | 0.5 kΩ |
| F3 | R2 | 3 kΩ | R2+50% | 4.5 kΩ |
| F4 | R2 | 3 kΩ | R2-50% | 1.5 kΩ |
| F5 | R3 | 1 kΩ | R3+50% | 1.5 kΩ |
| F6 | R3 | 1 kΩ | R3-50% | 0.5 kΩ |
| F7 | C1 | 5nf | C1+50% | 7.5 nF |
| F8 | C1 | 5 nF | C1-50% | 2.5 nF |
| F9 | C2 | 5 nF | C2+50% | 7.5 nF |
| F10 | C2 | 5 nF | C2-50% | 2.5 nF |

### 4.1. First circuit: a Sallen–Key band-pass filter

The first CUT used in this paper is a Sallen–Key band-pass filter [2] (Fig. 4). The resistors and capacitors tolerance values are set to 5% and 10%, respectively.

In this experiment circuit, we use the single pulse of 5 V pick amplitude and duration of 10 μs which have been adopted in Ref. [2] as input of the CUT in time domain. An AC signal with magnitude of 5 V is used as input of the CUT in the frequency domain. A transient and an AC signal analysis have been carried out under PSPICE simulator in order to obtain frequency and time domain responses. Therefore, the nominal and the fault values of components are shown in Table 1. The fault classes include

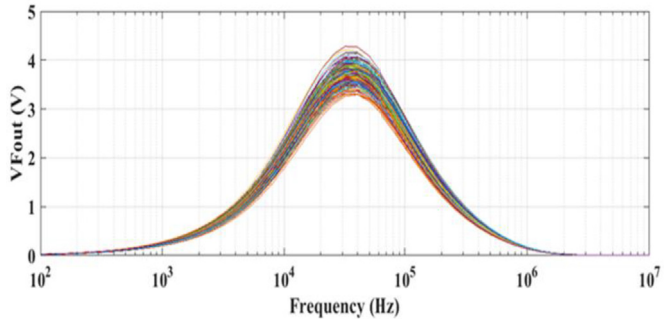


**Fig. 5.** The fault free CUT Frequency response using Monte-Carlo simulation for 200 runs.

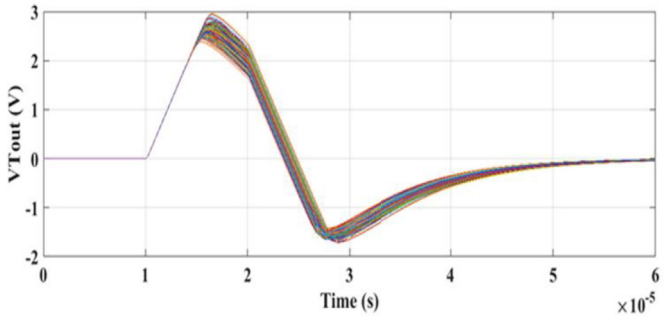


**Fig. 6.** The fault free CUT transient response using Monte-Carlo simulation for 200 runs.

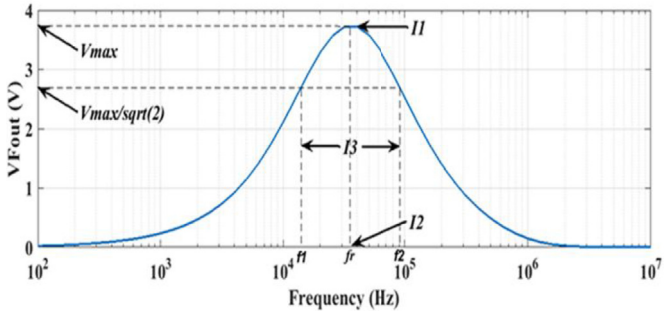


**Fig. 7.** Features extraction of the fault free CUT frequency response.

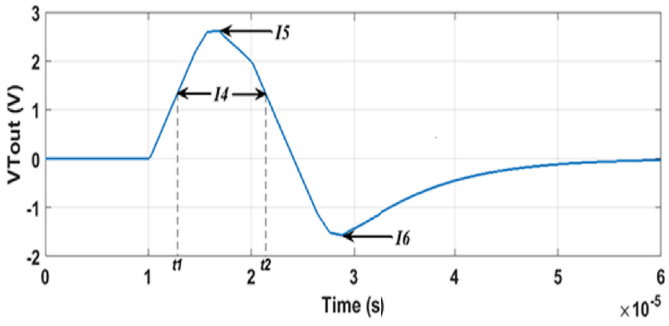


**Fig. 8.** Features extraction of the fault free CUT transient response.

R1, R2, R3, C1 and C2 values varied by 50% lower and higher than their nominal values and fault free class (FF).

In order to generate the simulation fault data according to the fault classes in Table 1, a frequency domain analysis, time domain transient analysis and Monte Carlo analysis using ORCAD software are used [18]. Therefore, the simulated data for each fault class are 200 sets. Then, 200 original samples for each fault class are divided into 100 training feature vectors and 100 testing samples.

#### 4.1.1. Simulation results

The frequency response of the fault free CUT is represented in Fig. 5 and the transient response curve is represented in Fig. 6.

#### 4.1.2. Features generation

Feature generation is a process which makes a map from raw data to the classifier input. This is aimed to build more efficient features for fault detection and classification task.

From the frequency and the transient responses presented in Figs. 7 and 8, features: I1, I2, I3, I4, I5 and I6 were extracted for both healthy and faulty CUT using the following formulas:

a. Feature 1: Frequency response maximum amplitude (I1)

This first classifier feature represents the pick or the maximum value of the frequency response curve.

$$I_1 = \max(VF_{out}) \tag{15}$$

b. Feature 2: center frequency (I2)

The center frequency represents the midpoint frequency in between the -3 dB cutoff frequencies of a band pass filter. The -3 dB cutoff points are also referred to as the lower cutoff frequency (f1) and upper cutoff frequency (f2) of a filter.

$$I_2 = f_r = \frac{f_1 + f_2}{2} \tag{16}$$

c. Feature 3: Bandwidth (I3)

The bandwidth (BW) is the difference between lower and upper cut-off frequencies (f1 and f2).

$$I_3 = f2 - f1 \tag{17}$$

d. Feature 4: Transient response pulse width (I4)

The pulse width (PW) is the elapsed time between the rising and the falling edges (t1, t2) of the transient response. To make this measurement repeatable and accurate, we use the 50% power level as the reference point.

$$I_4 = t2 - t1 \tag{18}$$

e. Feature 5: Transient response maximum point (I5)

This feature represents the maximum point value of the transient trace.

$$I_5 = \max(VT_{out}) \tag{19}$$

f. Feature 6: Transient response minimum point (I6)

This feature is chosen as the maximum value of the transient trace.

$$I_6 = \min(VT_{out}) \tag{20}$$

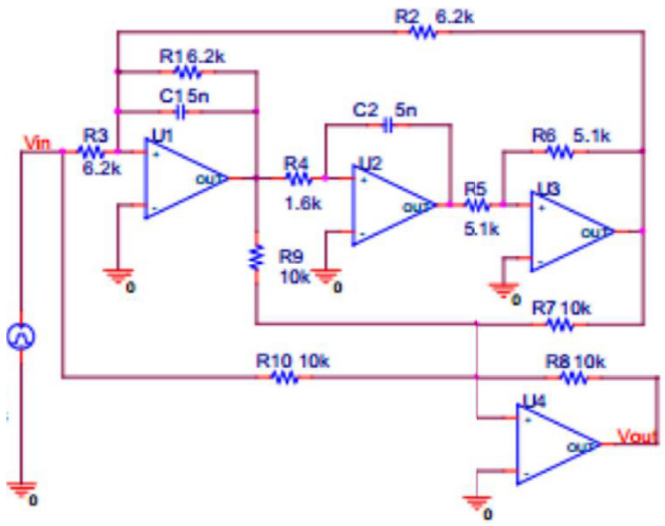


**Fig. 9.** Four opamp biquad high-pass filter.

**Table 2**
Nominal and fault values for a four opamp biquad high-pass filter.

| Fault ID | Element | Nominal value | Fault type | Faulty value |
|---|---|---|---|---|
| F0 | – | – | FF | – |
| F1 | R1 | 6.2 kΩ | R1+50% | 9.3 kΩ |
| F2 | R1 | 6.2 kΩ | R1-50% | 3.1 kΩ |
| F3 | R2 | 6.2 kΩ | R2+50% | 9.3 kΩ |
| F4 | R2 | 6.2 kΩ | R2-50% | 3.1 kΩ |
| F5 | R3 | 6.2 kΩ | R3+50% | 9.3 kΩ |
| F6 | R3 | 6.2 kΩ | R3-50% | 3.1 kΩ |
| F7 | R4 | 1.6 kΩ | R4+50% | 2.4 kΩ |
| F8 | R4 | 1.6 kΩ | R4-50% | 0.8 kΩ |
| F9 | C1 | 5 nF | C1+50% | 7.5 nF |
| F10 | C1 | 5 nF | C1-50% | 2.5 nF |
| F11 | C2 | 5 nF | C2+50% | 7.5 nF |
| F12 | C2 | 5 nF | C2-50% | 2.5 nF |

### 4.2. Second circuit: a four opamp biquad high-pass filter

The second example circuit to be tested is a four opamp biquad high-pass filter, which is used as a CUT in Ref. [2]. The nominal values of all the components are shown in Fig. 9. Inputs signals are also single pulse of 5 V pick amplitude and duration of 10 μs in time domain, and an AC signal with magnitude of 5 V in the frequency domain. The circuit simulation has been run under the same software as the first circuit for both transient and AC analysis. The tolerance of resistors and capacitors are set to 5% and 10%, respectively. The nominal and the fault values of components are shown in Table 2. Therefore, in the experiment, the transient and the frequency responses have been collected for 12 single faulty and fault free (FF) circuit to verify our proposed method's accuracy. These selected faults are dealt with the fault classes that include R1, R2, R3, R4, C1 and C2 whose nominal values are varied by less and more than 50%.

### 4.3. Third circuit: a leapfrog filter

The third example circuit to be tested is a leapfrog filter, which is designed with Current Feedback Operational Amplifiers (CFOAs). The nominal value of each component is labeled in Fig. 10 and the tolerance of resistors and capacitors are set as 5% and 10%, respectively. Inputs signals are sinusoidal signal of 5 V pick amplitude and frequency of 1 KHZ in time domain, and an AC signal with magnitude of 5 V in the frequency domain. Therefore, in this experiment, 24 single fault cases are selected to verify our proposed method's classification accuracy. Fault classes are shown in Table 3.

## 5. Experimental results and discussion

In this section, we exhibit firstly the proposed method for feature dimensionality reduction is proposed and its application to the group of classifiers relating to an appropriate circuit. We enumerate 10 classifiers for the first CUT, 12 classifiers for the second CUT and 24 classifiers for the third CUT. Then, the proposed multi-class neuro-fuzzy classifier was trained and tested with the reduced whole original feature space, which is defined by a vector of all features. Finally, the proposed classifier will be compared to an ANN classifier and the method based on statistical property features in fractional domain based on FRFT proposed in Ref. [2].

### 5.1. Results for the Sallen-Key band pass filter

*a. Classifier Features reduction*

Features selection is an important stage for each classifier. Whereas, constructed features have the same effect on the classifier performance. So, the reducing of feature dimensionality is more needed. This process step leads to evade redundant information, and also eliminating features that have no effect on the classifier decision. For these reasons, a feature dimensionality reduction technique is applied to pick the best features set, and cuts down dimensionality of the classifier input.

An algorithm is developed to choose automatically a subset of features that will be used for training and testing the classifier. Then, the built model will be stored with its performance for further usage. This process is repeated until all features combinations are generated. Finally, all classifier performances are compared, and the features will be retained for a specified fault type classification as illustrated in Table 4 bellow.

An ANFIS classifier was built for each combination, the obtained classifiers are performed according to their RMS error, and the most appropriate combination predicting the classifier output is retained.

In this study, ten classifiers are considered for the Sallen-Key band-pass filter: ANFIS-1 (F1 classifier), ANFIS-2 (F2 classifier), ANFIS-3 (F3 classifier), ANFIS-4 (F4 classifier), ANFIS-5 (F5 classifier), ANFIS-6 (F6 classifier), ANFIS-7 (F7 classifier), ANFIS-8 (F8 classifier), ANFIS-9 (F9 classifier) and ANFIS-10 (F10 classifier). The best combination of features is selected for each one of them, as shown in Table 4 (Bold number indicate the optimal values of RMSE and the best selected combination of features).

From the Table 4, results of selecting classifiers inputs are presented. The best combination of features has been hold for the classifier evaluation. We can clearly see that the training and the testing errors are reduced by increasing the selected features number. Therefore for some classifiers, increasing the number of features from 3 to 4 does not minimize much the training and the testing errors. Thus, this will neither achieve the classification efficiency nor improve the classification accuracy. For these reasons, only three features will be selected for these classifiers and which are ANFIS-2, ANFIS-8 and ANFIS-10.

*b. ANFIS Membership function type and number optimization*

After features selection step, an efficient method has been adopted to select the best ANFIS model, based on the decreasing of Root Mean Square Error (RMSE), and increasing the accuracy of the considered architecture for each classifier.

The main parts of the multiclass neuro-fuzzy classifier to be designed consist of the membership functions type (triangular, trapezoidal, generalized bell-shaped, Gaussian, Pi-shaped curve and Dsig-shaped curve). The classifier output is a linear combination of its inputs (Sugeno fuzzy inference system) [20]. During the optimization process, different built-in membership functions (MFs) types has been involved to choose the most appropriate one for the classifier model development as shown in Table 5 below.

The optimized membership function types and number for each classifier are presented in Table 6 bellow:

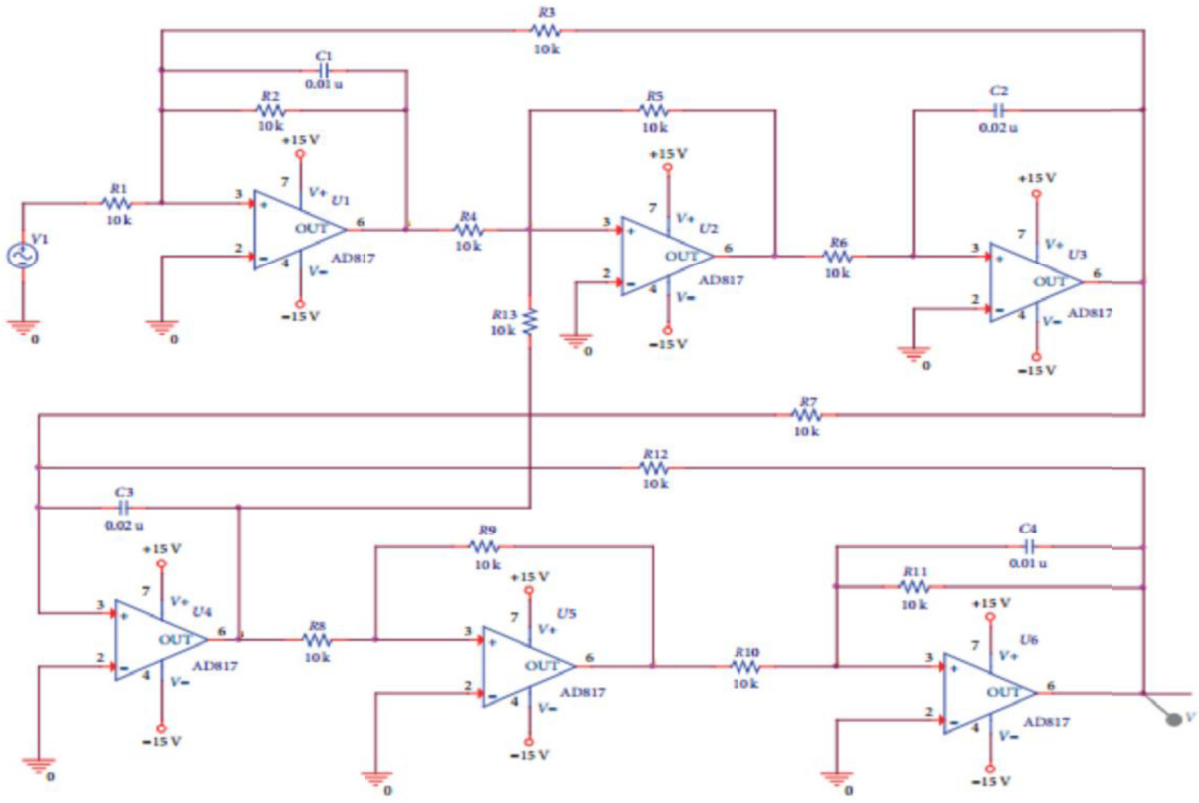


**Fig. 10.** A leapfrog filter circuit.

**Table 3**
Nominal and fault values for a leapfrog filter.

| Fault ID | Element | Nominal value | Fault type | Faulty value |
|---|---|---|---|---|
| F0 | – | – | FF | – |
| F1 | R1 | 10 kΩ | R1-50% | 5 kΩ |
| F2 | R1 | 10 kΩ | R1+50% | 15 kΩ |
| F3 | R2 | 10 kΩ | R2-50% | 5 kΩ |
| F4 | R2 | 10 kΩ | R2+50% | 15 kΩ |
| F5 | R3 | 10 kΩ | R3-50% | 5 kΩ |
| F6 | R3 | 10 kΩ | R3+50% | 15 kΩ |
| F7 | R4 | 10 kΩ | R4-50% | 5 kΩ |
| F8 | R4 | 10 kΩ | R4+50% | 15 kΩ |
| F9 | R6 | 10 kΩ | R6-50% | 5 kΩ |
| F10 | R6 | 10 kΩ | R6+50% | 15 kΩ |
| F11 | R7 | 10 kΩ | R7-50% | 5 kΩ |
| F12 | R7 | 10 kΩ | R7+50% | 15 kΩ |
| F13 | R8 | 10 kΩ | R8-50% | 5 kΩ |
| F14 | R8 | 10 kΩ | R8+50% | 15 kΩ |
| F15 | R10 | 10 kΩ | R10-50% | 5 kΩ |
| F16 | R10 | 10 kΩ | R10 + 50% | 15 kΩ |
| F17 | C1 | 10 nF | C1-50% | 5 nF |
| F18 | C1 | 10 nF | C1+50% | 15 nF |
| F19 | C2 | 20 nF | C2-50% | 10 nF |
| F20 | C2 | 20 nF | C2+50% | 30 nF |
| F21 | C3 | 20 nF | C3-50% | 10 nF |
| F22 | C3 | 20 nF | C3+50% | 30 nF |
| F23 | C4 | 10 nF | C4-50% | 5 nF |
| F24 | C4 | 10 nF | C4+50% | 15 nF |

For the first circuit to test, the best membership function for each classifier is as follows:

- ANFIS 1: generalized bell-shaped membership function with number of three.
- ANFIS 2: Gaussian membership functions with number of four.
- ANFIS 3: Pi-shaped membership functions with number of three.
- ANFIS 4: generalized bell-shaped membership function with number of four.
- ANFIS 5: triangle-shaped membership functions with number of four.
- ANFIS 6: generalized bell-shaped membership function with number of four.
- ANFIS 7: Trapezoidal membership functions with number of four.
- ANFIS 8: Gaussian membership functions with number of four.
- ANFIS 9: triangle-shaped membership functions with number of four.
- ANFIS 10: Gaussian membership functions with number of four.

*c. Fault Classification with artificial neural network (ANN) classifier*

For comparisons purpose, the designed multiclass neuro-fuzzy classifier has been compared to the artificial neural network (ANN) one (See Table 7), which is a multilayer feed-forward perception (MLP) with one hidden layer. For fast optimization of the network, a Levenberg-Marquardt (LM) back-propagation algorithm has been applied (Fig. 11).

This comparison shows clearly the superiority of the neuro-fuzzy classifier over traditional ANN-classifier. Moreover, the proposed classifier can be used to further improve these important results as it shown in Table 7.

The comparison of the classification accuracy with method used in Ref. [2] and ANN classifier is presented in Table 8, from which it can be concluded that the proposed classifier has a better gratitude capability.

From the comparison between the three methods, it is thus clear that the proposed method based on neuro-fuzzy classifier has produced the best classification accuracy for the major classifiers (from F3 to F10), which has an average equal to 99.76%. However, the method using in Ref. [2] and the ANN method have provided classification accuracy averages of 98.57% and 97.42% respectively.

### 5.2. Results for the four opamp biquad high-pass filter

All the test steps being followed with the first circuit are applied to test the four opamp biquad high pass filter to prove the classification

**Table 4**
Features selection for classifiers of the Sallen_Key band pass filter.

| ANFIS-NB | Total number of features | 6 | 6 | 6 | 6 |
|---|---|---|---|---|---|
| | Selected features | 1 | 2 | 3 | 4 |
| ANFIS-1 | RMSE (Training) | 0.1716 | 0.0901 | 0.0621 | 0.0371 |
| | RMSE (Testing) | 0.1789 | 0.0912 | **0.0671** | 0.0477 |
| | Best combination of features | I1 | I3 I6 | **I1 I3 I6** | I1 I2 I3 I5 |
| ANFIS-2 | RMSE (Training) | 0.2543 | 0.1542 | 0.1383 | 0.1009 |
| | RMSE (Testing) | 0.2555 | 0.1590 | 0.1459 | **0.1082** |
| | Best combination of features | I5 | I2 I5 | I2 I4 I6 | **I2 I4 I5 I6** |
| ANFIS-3 | RMSE (Training) | 0.2396 | 0.0719 | 0.0309 | 0.0154 |
| | RMSE (Testing) | 0.2409 | 0.0732 | **0.0368** | 0.0242 |
| | Best combination of features | I2 | I2 I3 | **I2 I5 I6** | I1 I2 I5 I6 |
| ANFIS-4 | RMSE (Training) | 0.2192 | 0.1200 | 0.0630 | 0.0481 |
| | RMSE (Testing) | 0.2215 | 0.1230 | **0.0770** | 0.0621 |
| | Best combination of features | I3 | I2 I3 | **I1 I2 I3** | I1 I3 I5 I6 |
| ANFIS-5 | RMSE (Training) | 0.1441 | 0.0446 | 0.0187 | 0.0114 |
| | RMSE (Testing) | 0.1427 | 0.0495 | **0.0188** | 0.0137 |
| | Best combination of features | I3 | I3 I6 | **I2 I3 I6** | I1 I2 I5 I6 |
| ANFIS-6 | RMSE (Training) | 0.1715 | 0.0999 | 0.0495 | 0.0326 |
| | RMSE (Testing) | 0.1806 | 0.1072 | **0.0598** | 0.0410 |
| | Best combination of features | I5 | I2 I6 | **I1 I5 I6** | I1 I2 I5 I6 |
| ANFIS-7 | RMSE (Training) | 0.2552 | 0.0839 | 0.0596 | 0.0314 |
| | RMSE (Testing) | 0.2550 | 0.0890 | **0.0612** | 0.0456 |
| | Best combination of features | I3 | I1 I3 | **I1 I3 I6** | I1 I2 I3 I5 |
| ANFIS-8 | RMSE (Training) | 0.2627 | 0.1676 | 0.1294 | 0.0951 |
| | RMSE (Testing) | 0.2610 | 0.1764 | 0.1343 | **0.1083** |
| | Best combination of features | I5 | I2 I5 | I3 I4 I6 | **I2 I4 I5 I6** |
| ANFIS-9 | RMSE (Training) | 0.2542 | 0.0722 | 0.0241 | 0.0138 |
| | RMSE (Testing) | 0.2554 | 0.0721 | **0.0232** | 0.0165 |
| | Best combination of features | I3 | I5 I6 | **I1 I2 I3** | I1 I2 I3 I6 |
| ANFIS-10 | RMSE (Training) | 0.2613 | 0.0998 | 0.0766 | 0.0462 |
| | RMSE (Testing) | 0.2642 | 0.1012 | 0.0821 | **0.0624** |
| | Best combination of features | I3 | I5 I6 | I1 I2 I3 | **I1 I2 I3 I6** |

**Table 5**
RMS Errors and membership function types during the optimization process.

| MF-MFN | MF type description | RMS error for testing | | | | |
|---|---|---|---|---|---|---|
| | | Anflis-1 | Anfis-2 | Anfis-3 | Anfis-4 | Anfis-5 |
| Trimf-2 | Triangle curve | 0.0643 | 0.1879 | 0.0793 | 0.2243 | 0.0418 |
| Trimf-3 | | 0.0753 | 0.1410 | 0.0429 | 0.0967 | 0.0243 |
| Trimf-4 | | 0.0581 | 0.1125 | 0.0313 | 0.0728 | 0.0068 |
| Trapmf-2 | Trapezoidal curve | 0.0454 | 0.1750 | 0.0375 | 0.2288 | 0.0652 |
| Trapmf-3 | | 0.0522 | 0.1520 | 0.0743 | 0.0979 | 0.0279 |
| Trapmf-4 | | 0.0453 | 0.1322 | 0.0190 | 0.0839 | 0.0600 |
| Gbellmf-2 | Generalized bell curve | 0.0850 | 0.1728 | 0.0503 | 0.1316 | 0.0422 |
| Gbellmf-3 | | 0.0362 | 0.1309 | 0.0506 | 0.0655 | 0.0170 |
| Gbellmf-4 | | 0.0470 | 0.1066 | 0.0261 | 0.0621 | 0.0267 |
| Gaussmf-2 | Gaussian curve | 0.0909 | 0.1791 | 0.0480 | 0.1748 | 0.0295 |
| Gaussmf-3 | | 0.0429 | 0.1165 | 0.0447 | 0.0815 | 0.0254 |
| Gaussmf-4 | | 0.0453 | 0.1010 | 0.0197 | 0.0673 | 0.0169 |
| Pimf-2 | Pi-shaped curve | 0.0553 | 0.1779 | 0.0288 | 0.2451 | 0.1138 |
| Pimf-3 | | 0.0603 | 0.1798 | 0.0862 | 0.0971 | 0.0414 |
| Pimf-4 | | 0.0480 | 0.1966 | 0.0090 | 0.0862 | 0.0727 |
| Dsigmf-2 | Dsig-shaped curve | 0.0751 | 0.1791 | 0.1529 | 0.2202 | 0.1499 |
| Dsigmf-3 | | 0.0562 | 0.1583 | 0.1350 | 0.1155 | 0.0284 |
| Dsigmf-4 | | 0.0576 | 0.1458 | 0.0667 | 0.1054 | 0.0489 |
| | | Anflis-6 | Anfis-7 | Anfis-8 | Anfis-9 | Anfis-10 |
| Trimf-2 | Triangle curve | 0.1018 | 0.0946 | 0.1788 | 0.0895 | 0.1304 |
| Trimf-3 | | 0.0617 | 0.0598 | 0.1324 | 0.0279 | 0.0684 |
| Trimf-4 | | 0.0917 | 0.0858 | 0.1112 | 0.0159 | 0.0758 |
| Trapmf-2 | Trapeizoidal curve | 0.1014 | 0.0758 | 0.1878 | 0.0752 | 0.0778 |
| Trapmf-3 | | 0.0700 | 0.0547 | 0.1434 | 0.0433 | 0.5470 |
| Trapmf-4 | | 0.0642 | 0.0215 | 0.1230 | 0.0406 | 0.0734 |
| Gbellmf-2 | Generalized bell curve | 0.0727 | 0.0807 | 0.1744 | 0.0433 | 0.0739 |
| Gbellmf-3 | | 0.0438 | 0.0535 | 0.1284 | 0.0281 | 0.0527 |
| Gbellmf-4 | | 0.0403 | 0.0344 | 0.1072 | 0.0228 | 0.0550 |
| Gaussmf-2 | Gaussian curve | 0.0847 | 0.0966 | 0.1944 | 0.0390 | 0.0866 |
| Gaussmf-3 | | 0.0442 | 0.0721 | 0.1130 | 0.0225 | 0.0509 |
| Gaussmf-4 | | 0.0477 | 0.0400 | 0.1014 | 0.0215 | 0.0516 |
| Pimf-2 | Pi-shaped curve | 0.1292 | 0.1816 | 0.1803 | 0.1352 | 0.0738 |
| Pimf-3 | | 0.0657 | 0.0747 | 0.2188 | 0.0508 | 0.1525 |
| Pimf-4 | | 0.0646 | 0.0251 | 0.1706 | 0.0455 | 0.0800 |
| Dsigmf-2 | Dsig-shaped curve | 0.1269 | 0.1728 | 0.1815 | 0.1429 | 0.1280 |
| Dsigmf-3 | | 0.0661 | 0.0790 | 0.1912 | 0.0915 | 0.1246 |
| Dsigmf-4 | | 0.0658 | 0.0536 | 0.1321 | 0.0391 | 0.0878 |

**Table 6**
Optimized membership function type and number.

| ANFIS-NB | MF-MFN | RMS error for testing |
|---|---|---|
| ANFIS-1 | Gbellmf-3 | 0.0362 |
| ANFIS-2 | Gaussmf-4 | 0.1010 |
| ANFIS-3 | Pimf-4 | 0.0090 |
| ANFIS-4 | Gbellmf-4 | 0.0621 |
| ANFIS-5 | Trimf-4 | 0.0068 |
| ANFIS-6 | Gbellmf-4 | 0.0403 |
| ANFIS-7 | Trapmf-4 | 0.0215 |
| ANFIS-8 | Gaussmf-4 | 0.1014 |
| ANFIS-9 | Trimf-4 | 0.0159 |
| ANFIS-10 | Gaussmf-3 | 0.0509 |

accuracy of the proposed classifier. First, the features selection technique is applied to choose the best combinations of features for each classifier. Then, membership function types are optimized to choose the optimal type of membership function for each classifier. Finally, classifiers are trained to test our approach. Table 9 depicts the comparison results between the proposed method and ANN classifier. The obtained results show the high accuracy of the ANFIS classifier over the ANN classifier.

Table 10 shows the comparison results between the proposed classifier (ANFIS), ANN classifier and the method based on statistical property features in fractional domain based on FRFT proposed in Ref. [2].

### 5.3. Results for the leapfrog filter

The obtained results when testing the leapfrog filter are shown in Table 11. The average classification accuracy of our method is 97.52%, whereas for the method using ANN classifier, the average classification accuracy is 96.39%.

Therefore, we can see that the proposed method is better than the other classification methods for single faults in the leapfrog filter circuit. Once again, it is clear enough that our classifier method shows great efficiency of diagnostic accuracies and can cope with any analog filtering circuit.

## 6. Conclusion

In this paper, an adaptive multiclass neuro-fuzzy classifier and features reduction technique for faults classification in analog integrated circuits is proposed. The effectiveness of the proposed method has been validated through a Sallen-Key band pass filter, a four opamp biquad high-pass filter and a leapfrog filter, for single parametric faults classification. Experiments for the three circuits have been performed to evaluate the appreciation capability of the proposed classifier. Experiment's results have been compared to those of both the artificial neural network (ANN) classification method and the method using statistical property features of transformed signals by FRFT in the optimal fractional order domain, as features too. Consequently, the proposed method has demonstrated the highest accuracy in terms of fault classification. The average accuracy is about 99.76% and 96.74% and 97.52% for the three CUTs mentioned above respectively. Furthermore, the use of ANFIS classification based on features reduction technique has conducted to

**Table 7**
Comparison between multiclass neuro fuzzy and ANN classifiers for Sallen Key band pass filter.

| Fault ID | RMS error | | $R^2$ | | Classification accuracy (%) | |
|---|---|---|---|---|---|---|
| | ANFIS | ANN | ANFIS | ANN | ANFIS | ANN |
| F1 | 0.1010 | 0.1853 | 0.8979 | 0.6566 | 99.20 | 95.80 |
| F2 | 0.0362 | 0.0632 | 0.9868 | 0.9600 | 99.90 | 99.50 |
| F3 | 0.0621 | 0.2667 | 0.9586 | 0.2885 | 99.60 | 90.00 |
| F4 | 0.0090 | 0.1719 | 0.9991 | 0.7043 | 100.00 | 96.40 |
| F5 | 0.0430 | 0.0039 | 0.9837 | 0.9998 | 99.90 | 100.00 |
| F6 | 0.0068 | 0.0009 | 0.9995 | 1.0000 | 100.00 | 100.00 |
| F7 | 0.1014 | 0.1162 | 0.8970 | 0.8649 | 99.20 | 98.30 |
| F8 | 0.0215 | 0.1895 | 0.9953 | 0.6409 | 100.00 | 95.20 |
| F9 | 0.0509 | 0.0860 | 0.9740 | 0.9260 | 99.80 | 99.10 |
| F10 | 0.0159 | 0.0245 | 0.9974 | 0.9940 | 100.00 | 99.90 |
| Average accuracy | | | | | **99.76** | **97.42** |

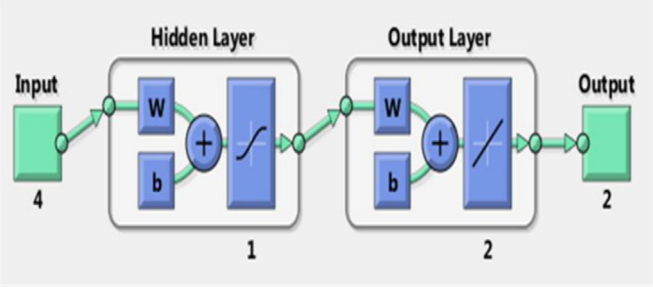


**Fig. 11.** Artificial neuronal networks (ANN) diagram.

**Table 8**
Comparison of the classification accuracy between the proposed method and other methods for the Sallen Key band pass filter.

| Fault ID | Classification accuracy (%) | | |
|---|---|---|---|
| | ANFIS | ANN | Method [2] |
| F1 | 99.20 | 95.80 | – |
| F2 | 99.90 | 99.50 | – |
| F3 | 99.60 | 90.00 | 98.00 |
| F4 | 100.00 | 96.40 | 100.00 |
| F5 | 99.90 | 100.00 | 100.00 |
| F6 | 100.00 | 100.00 | 98.57 |
| F7 | 99.20 | 98.30 | 99.00 |
| F8 | 100.00 | 95.20 | 100.00 |
| F9 | 99.80 | 99.10 | 96.00 |
| F10 | 100.00 | 99.90 | 97.00 |
| **average** | **99.76** | **97.42** | **98.57** |

**Table 9**
Comparison between multiclass neuro fuzzy and ANN classifiers for a four opamp biquad high pass filter.

| Fault ID | RMS error | | $R^2$ | | Classification accuracy (%) | |
|---|---|---|---|---|---|---|
| | ANFIS | ANN | ANFIS | ANN | ANFIS | ANN |
| F1 | 0.1354 | 0.0715 | 0.7798 | 0.9387 | 99.41 | 99.33 |
| F2 | 0.1431 | 0.2050 | 0.7542 | 0.4953 | 98.67 | 91.66 |
| F3 | 0.2194 | 0.2109 | 0.4223 | 0.4662 | 91.58 | 91.33 |
| F4 | 0.2072 | 0.2060 | 0.4847 | 0.4906 | 91.75 | 91.85 |
| F5 | 0.1215 | 0.2886 | 0.9465 | 0.9820 | 99.66 | 91.66 |
| F6 | 0.0582 | 0.0115 | 0.9592 | 0.9984 | 100.00 | 100.00 |
| F7 | 0.1195 | 0.1867 | 0.8284 | 0.5817 | 99.91 | 95.25 |
| F8 | 0.1281 | 0.0485 | 0.8029 | 0.9719 | 99.58 | 99.50 |
| F9 | 0.1814 | 0.2145 | 0.6047 | 0.4477 | 96.91 | 90.25 |
| F10 | 0.0298 | 0.0054 | 0.9893 | 1.0000 | 100.00 | 100.00 |
| F11 | 0.2162 | 0.2145 | 0.4389 | 0.4478 | 92.33 | 92.25 |
| F12 | 0.2089 | 0.2066 | 0.4766 | 0.4875 | 91.16 | 91.66 |
| Accuracy average | | | | | **96.74** | **94.53** |

**Table 10**
Comparison of the classification accuracy between the proposed method and other methods for the four opamp high pass filter.

| Fault ID | Classification accuracy (%) | | |
|---|---|---|---|
| | ANFIS | ANN | Method [2] |
| F1 | 99.66 | 91.66 | 81.00 |
| F2 | 100.00 | 100.00 | 100.00 |
| F3 | 99.91 | 95.25 | 89.70 |
| F4 | 99.58 | 99.50 | 90.00 |
| F5 | 96.91 | 90.25 | 98.00 |
| F6 | 100.00 | 100.00 | 100.00 |
| F7 | 92.33 | 92.25 | 89.60 |
| F8 | 91.16 | 91.66 | 100.00 |
| F9 | 99.41 | 99.33 | 90.00 |
| F10 | 98.67 | 91.66 | 100.00 |
| F11 | 91.58 | 91.33 | 100.00 |
| F12 | 91.75 | 91.85 | 100.00 |
| **average** | **96.74** | **94.53** | **94.85** |

**Table 11**
Comparison between multiclass neuro fuzzy and ANN classifiers for the leapfrog filter.

| Fault ID | RMS error | | $R^2$ | | Classification accuracy (%) | |
|---|---|---|---|---|---|---|
| | ANFIS | ANN | ANFIS | ANN | ANFIS | ANN |
| F1 | 0.0003 | 0.0002 | 1.0000 | 1.0000 | 100.00 | 100.00 |
| F2 | 0.1488 | 0.1691 | 0.4682 | 0.3136 | 97.41 | 95.83 |
| F3 | 0.1053 | 0.0908 | 0.7337 | 0.8017 | 99.25 | 97.00 |
| F4 | 0.1335 | 0.1738 | 0.5721 | 0.2745 | 98.75 | 95.83 |
| F5 | 0.0703 | 0.0583 | 0.9812 | 0.9182 | 100.00 | 99.08 |
| F6 | 0.1552 | 0.1970 | 0.4212 | 0.0677 | 97.25 | 95.83 |
| F7 | 0.0499 | 0.0658 | 0.9400 | 0.8959 | 100.00 | 99.00 |
| F8 | 0.1237 | 0.1774 | 0.6324 | 0.2446 | 98.33 | 95.83 |
| F9 | 0.0969 | 0.0866 | 0.7745 | 0.8197 | 100.00 | 99.08 |
| F10 | 0.1839 | 0.1916 | 0.1881 | 0.1187 | 95.83 | 95.83 |
| F11 | 0.0764 | 0.0615 | 0.8597 | 0.9090 | 99.75 | 99.00 |
| F12 | 0.1813 | 0.1875 | 0.2104 | 0.1556 | 95.83 | 95.83 |
| F13 | 0.1712 | 0.1809 | 0.2965 | 0.2146 | 95.66 | 95.83 |
| F14 | 0.1015 | 0.0964 | 0.7526 | 0.7766 | 99.83 | 98.83 |
| F15 | 0.1568 | 0.1813 | 0.4099 | 0.2104 | 96.33 | 95.83 |
| F16 | 0.1486 | 0.1895 | 0.4697 | 0.1381 | 97.08 | 95.83 |
| F17 | 0.1787 | 0.1952 | 0.2335 | 0.0847 | 95.83 | 95.83 |
| F18 | 0.1784 | 0.1982 | 0.2358 | 0.0751 | 95.83 | 92.25 |
| F19 | 0.1889 | 0.1981 | 0.1432 | 0.0577 | 95.83 | 95.83 |
| F20 | 0.1657 | 0.1998 | 0.3405 | 0.0414 | 95.66 | 91.83 |
| F21 | 0.1863 | 0.1984 | 0.1664 | 0.0549 | 95.75 | 95.66 |
| F22 | 0.1653 | 0.1602 | 0.3436 | 0.3840 | 95.66 | 95.91 |
| F23 | 0.1798 | 0.1982 | 0.2238 | 0.0566 | 95.83 | 95.83 |
| F24 | 0.1474 | 0.1996 | 0.4782 | 0.0431 | 98.83 | 95.83 |
| Accuracy average | | | | | **97.52** | **96.39** |

single parametric faults analog circuits' diagnosis improvement in terms of data compression. Once again, the proposed method has achieved a high level of efficiency of performance comparing to the aforementioned ones. Therefore, the results encourage the use of ANFIS method to be involved with other faults types such as double faults and catastrophic faults. This will probably provide solutions to the analog fault diagnosis problems and enhance the analog integrated circuits test efficiency.

## References

[1] D. Binu, B.S. Kariyappa, A survey on fault diagnosis of analog circuits: taxonomy and state of the art, AEU-Int. J. Electr. Commun. 73 (2017) 68–83.
[2] P. Song, Y. He, Statistical property feature extraction based on FRFT for fault diagnosis of analog circuits, Analog Integr. Circuits Signal Process. 87 (2016) 427–436.
[3] M. El-Gamal, S. El-Tantawy, Fuzzy inference system and neuro-fuzzy systems for analog fault diagnosis, Elect. Eng. Res. 1 (4) (2013) 116–125.
[4] D. Grzechca, J. Rutkowski, Use of neuro-fuzzy system to time domain electronic circuits fault diagnosis, in: ICSC Congress on Computational Intelligence Methods and Applications, 2005.

[5] A. Kumar, A.P. Singh, Fuzzy classifier for fault diagnosis in analog electronic circuits, ISA (Instrum. Soc. Am.) Trans. 52 (2013) 816–824.
[6] H. Luo, Y. Wong, J. Cui, A SVDD approach of fuzzy classification for analog circuit fault diagnosis with FWT as preprocessor, Int. J. Experts Syst. Appl. 38 (2011) 10554–10561.
[7] S.V.M. Rao, K.S. Sundari, Optimized multi frequency approach to analog fault diagnosis using Monte Carlo analysis, Electr. Electron. Eng. 4 (2014) 25–30.
[8] J. Cui, Y.R. Wang, A novel approach of analog circuit fault diagnosis using support vector machines classifier, Measurement 44 (1) (2011) 281–289.
[9] P. Chen, L. Yuan, Y. He, S. Luo, An improved SVM classifier based on double chains quantum genetic algorithm and its application in analogue circuit diagnosis, Neurocomputing 211 (2016) 202–211.
[10] Y. Qin, J. Xing, Y. Mao, Weak transient fault feature extraction based on an optimized Morlet wavelet and kurtosis, Meas. Sci. Technol. 27 (8) (2016), 085003.
[11] W. He, Y. He, Q. Luo, C. Zhang, Fault diagnosis for analog circuits utilizing time-frequency features and improved VVRKFA, Meas. Sci. Technol. 29 (4) (2018), 045004.
[12] S. Anas, M.H. ElMahlawy, M.E.A. Gadallah, E.A. ElSamahy, Parametric fault detection of analogue circuits, Int. J. Comput. Appl. 96 (9) (2014) 14–23.
[13] S. Srimani, K. Ghosh, H. Rahaman, Parametric fault detection in analog circuits, A statistical approach, in: IEEE 25th Asian Test Symposium vol. 16, 2016, pp. 2377–5386.
[14] B. Han, J. Li, H. Wu, Diagnosis method for analog circuit hard fault and soft fault, Telkomnika 11 (9) (2013) 5420–5426.
[15] M. Jahangiri, F. Razaghian, Fault detection in analogue circuits using hybrid evolutionary algorithm and neural network, Analog Integr. Circuits Signal Process. 80 (2014) 551–556.
[16] A. Kavithamani, V. Manikandan, N. Devarajan, Fault detection of analog circuits using network parameters, J. Electron. Test. 28 (2012) 257–261.
[17] A. Kavithamani, V. Manikandan, N. Devarajan, Soft fault classification of analog circuits using network parameters and neural networks, J. Electron. Test. 29 (2013) 237–240.
[18] Pspice, Circuit Analysis User's Guide, The Microsim Corp., CA, USA, 1992.
[19] M.F. Møller, A scaled conjugate gradient algorithm for fast supervised learning, Neural Network. 6 (1993) 525–533.
[20] J.S.R. Jang, ANFIS: adaptive-network-based fuzzy inference system, in: IEEE Transactions on Systems, Man, and Cybernetics, vol. 23, 1993, pp. 665–685.